

Effect of nonequilibrium quasiparticle flow on SNS Josephson junctions

V. K. Kaplunenko, V. V. Ryazanov, and V. V. Shmidt

Institute of Solid-State Physics, Academy of Sciences of the USSR

(Submitted 24 April 1985)

Zh. Eksp. Teor. Fiz. **89**, 1389–1403 (October 1985)

Experiments have been carried out on the effect of a nonequilibrium flow of quasiparticles on the Josephson properties of a Ta-Cu-Ta SNS junction. A nonequilibrium quasiparticle flow can be set up at the junction because the thickness of the superconducting banks of the SNS sandwich is on the order of the depth to which the longitudinal electric field penetrates into the superconductor, and the sandwich is bracketed by thick plates of a normal metal. During the injection of quasiparticles into one of the superconducting banks of the SNS junction, Josephson generation is excited at the junction; the total current flowing across the junction is zero. The nonequilibrium quasiparticle current which flows across the SNS junction is several times the critical current I_c and has no direct effect on its Josephson characteristics. The appearance of a difference in the electrochemical potentials of the pairs and of Josephson generation at the junction is due exclusively to the flow of the superconducting current. The experimental results are analyzed on the basis of an equivalent circuit proposed for the junction by Kadin, Smith, and Skocpol [J. Low Temp. Phys. **38**, 497 (1980)], simplified somewhat for the case at hand. A study of the temperature dependence of the effects shows that at $T > 0.97T_c$ the nonequilibrium quasiparticle current in the normal Josephson intermediate layer of the junction does not depend on Andreev reflection processes at the NS interfaces. The scale time for electron-phonon energy relaxation in the tantalum used as the superconductor is estimated to be $\tau_e \approx 4.0 \cdot 10^{-1}$ s.

1. INTRODUCTION

Nonequilibrium effects in superconductors and superconducting systems have recently become the subject of active research. Of particular interest are processes involving the excitation of quasiparticle flows in superconductors. We now know that at temperatures close to the critical temperature the injection of quasiparticles from a normal metal into a superconductor is accompanied by the onset of a longitudinal electric field, which penetrates a characteristic distance l_E into the superconductor. The distance l_E may exceed both the coherence length $\xi(T)$ and the London penetration depth $\lambda(T)$ (see the review by Artemenko and Volkov¹). The part of the superconductor with the longitudinal electric field is in a nonequilibrium state, characterized by an imbalance between the populations of the electron and hole branches of the spectrum of elementary excitations of the superconductor (quasiparticle charge imbalance). Such a nonequilibrium state is manifested in observable effects such as an excess resistance of the NS interface,^{1,2} quasiparticle charge-imbalance waves (waves of a longitudinal electric field),^{3,4} and the appearance of a difference in the electrochemical potentials of Cooper pairs and quasiparticles.^{5,6}

Nonequilibrium processes with a longitudinal electric field may bring about the interaction and synchronization in a chain of closely spaced Josephson junctions.^{7,8} For example, when one of the weak links goes into a resistive state, a current of quasiparticles arises; this current can reach adjacent weak links if they lie within distances comparable to the penetration depth l_E of the longitudinal electric field. As a result, there may be changes in the characteristics of the Josephson junctions, and they may be synchronized by both the steady-state quasiparticle currents⁹ and the propagation

of quasiparticle charge-imbalance waves.¹⁰ There is accordingly considerable interest in studying the properties of a Josephson junction in the case in which a nonequilibrium quasiparticle current flows through its superconducting banks and the weak link.

In the present paper we use the term “nonequilibrium state” of the superconducting banks to refer exclusively to the so-called transverse (charge) nonequilibrium state,¹¹ i.e., a state characterized only by an imbalance between the populations of the branches of the quasiparticle spectrum, but with the energy gap the same as in the equilibrium state.

Experiments on thermoelectric effects in SNS Josephson junctions^{12–14} have shown that a quasiparticle current induced by a heat flux induces as a response a supercurrent which changes the phase difference between the wave functions of the S-electrodes. It turns out that a similar effect can be observed by exciting a nonequilibrium quasiparticle current across a junction by injecting quasiparticles into one of the superconducting banks.¹⁵ If the superconducting bank of an SNS Josephson sandwich is sufficiently thin (if its thickness is comparable to l_E), a certain number of the quasiparticles will not manage to convert into pairs. These quasiparticles pass through the junction. The total current through the junction, however, must be zero since in an injection experiment the current is drawn from the same bank into which it is injected. Consequently, a response supercurrent must arise at the junction in order to cancel the nonequilibrium quasiparticle current through the junction; this response supercurrent will change the phase difference between the superconducting banks.

Another question of much interest is determining whether the normal component of the current (the nonequilibrium quasiparticle current) can have a direct effect on the

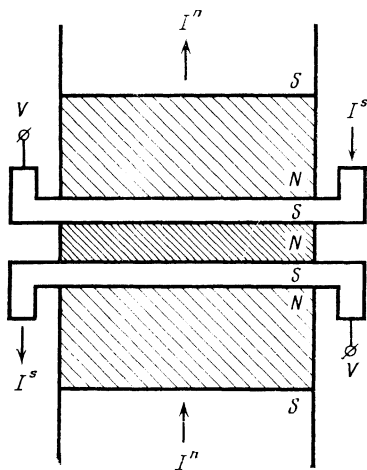


FIG. 1. Schematic diagram of the sample. The superconductor (S) is tantalum, and the normal metal (N) is copper. The thickness of the Josephson intermediate layer is $d_N \approx 5 \mu\text{m}$; the thickness of the tantalum superconducting plates is $d_S = 3\text{--}4 \mu\text{m}$; and the thickness of the other intermediate layers is greater than $50 \mu\text{m}$.

characteristics of a Josephson junction, e.g., Josephson vortices, if the junction is in an external magnetic field. A study of thermoelectric effects in Josephson junctions¹⁴ has revealed a Josephson generation excited exclusively by a heat flux. It has been shown that a heat flux causes a motion of Josephson vortices. Since the total electric current across the junction is zero in this case, it may be that only the supercurrent is acting on the Josephson vortices. This set of questions is the subject of the present study.

2. EXPERIMENTAL PROCEDURE AND FABRICATION OF THE SAMPLES

The Ta-Cu-Ta SNS Josephson junctions are fabricated by the method of joint hot rolling.¹⁶ Bulk metal stripes and foils are jointly rolled with slight compression at a temperature of about 900°C in a vacuum no worse than 10^{-5} Torr. The layers of the desired thickness are then produced by cold rolling under standard conditions. The samples are cut by an

electric-arc technique from the initial plate. The junctions are rectangular, with an area ranging from 1.5 to 2 mm^2 in the different samples. At a temperature $T \approx 0.994T_c$ the junctions typically have a critical current $I_c \approx 3 \cdot 10^{-5} \text{ A}$, a normal resistance $R_n \approx 2 \cdot 10^{-8} \Omega$, and a Josephson voltage $V_c = I_c R_n \approx 6 \cdot 10^{-13} \text{ V}$. At this temperature, the width of the junctions, $W = 1\text{--}2 \text{ mm}$, are roughly equal to the Josephson penetration depth λ_J .

Figure 1 is a schematic diagram of a test sample. The photograph in Fig. 2 is an enlarged image of the central part of the sample, including three intermediate layers of the Josephson junction. This photograph of the polished end of a sample was taken in a scanning electron microscope; the reference bar is $10 \mu\text{m}$ long. The copper Josephson intermediate layer of the SNS junction (the dark region in Fig. 2) has a thickness $d_N \approx 5 \mu\text{m}$ and is made of pure copper, in which the electron mean free path is comparable to the thickness of the intermediate layer. The superconducting plates of the junction (the lighter regions in Fig. 2) are made of tantalum foil with a resistance ratio $\rho(300 \text{ K})/\rho(4.5 \text{ K}) = 17$ ($T_c = 4.40 \text{ K}$). The thickness of these plates ranges from 3 to $4 \mu\text{m}$ in the different samples. The outer surfaces of the SNS sandwich are in good electric contact with the bulk copper layers, used to inject quasiparticles into the plates of the junction. The thickness of these layers is on the order of $50 \mu\text{m}$. On top of the copper layers there is also a tantalum superconducting coating, which is connected to the injection-current source and which is required to establish a uniform distribution of the quasiparticle current in the copper layer (the injection layer). The overall thickness of a sample is close to 1 mm . (The original multilayer sandwich prepared for the hot rolling is about 10 mm thick.) The quality and purity of the NS interfaces produced by this technique are discussed in Ref. 16.

The tantalum (superconducting) plates of the SNS junction extend from the sample in two opposite directions, as shown in Fig. 1. This configuration is produced by electric-arc cutting and by etching the copper in nitric acid. The niobium superconducting leads are attached to the thin tan-

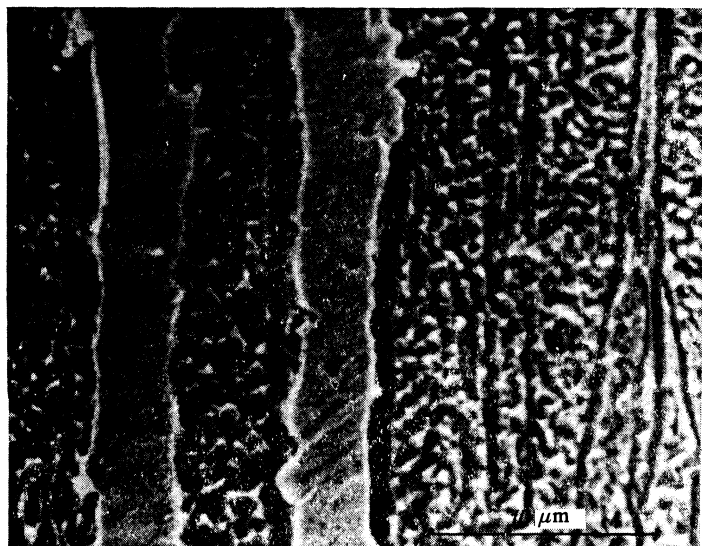


FIG. 2. Electron micrograph of the central part of sample No. 2. Dark regions—Copper; light regions—tantalum; reference bar— $10 \mu\text{m}$.

talium plates either by clamping or by spot welding in a vacuum of 10^{-5} Torr. In either case, the decrease in the value of T_c of the tantalum foil at the point of the attachment does not exceed 10^{-2} K, so that experiments can be carried in the immediate vicinity of T_c . A voltmeter connected to the superconducting plates of the junction measures the difference between the electrochemical potentials of the pairs across the junction. The voltage ($\sim 10^{-13} - 10^{-12}$ V) is measured with a sensitivity of $5 \cdot 10^{-14}$ V by means of an rf SQUID in an ordinary feedback circuit.

The temperature of the helium bath is stabilized near T_c of the tantalum (4.4 K), with a precision of almost $5 \cdot 10^{-4}$ K) by stabilizing the helium vapor pressure with a membrane monostat, whose comparison volume is in an auxiliary water constant-temperature bath. By adjusting the temperature of the comparison volume one can lower the temperature of the helium bath near T_c of the tantalum very smoothly.

In a study of the ordinary Josephson properties, the transport current is fed to the SNS junction directly through its superconducting plates. The voltage-current characteristic of one of the test junctions at $T \approx 0.994 T_c$ is shown by curve 2 in Fig. 3. The change in the critical current of junctions with the temperature near T_c corresponds to the established behavior $I_c \sim (1 - T/T_c)^2$. This behavior has been given a theoretical underpinning and has been verified experimentally¹⁷ for junctions with a thick pure *N* intermediate layer. The temperature dependence $I_c(T)$ at $T \ll T_c$ for Ta-Cu-Ta junctions fabricated by joint rolling and the quality of the *NS* interfaces of such junctions were discussed in Ref. 16.

It can be seen from Fig. 2 that the nonuniformity of the copper intermediate layer of the junctions is comparable to the coherence length ξ_n in pure copper ($\sim 0.4 \mu\text{m}$), so that the critical current density is noticeably nonuniform over the junction. The effect of this nonuniformity is discussed in Ref. 18. The nonuniformity seen in Fig. 2 may be amplified at the surface, however, during the grinding and subsequent etching of the sample. Despite a possible monotonic decrease in the thickness of the copper intermediate layer along the junction, the dependence of its critical current on the applied magnetic field shows that the supercurrent flows through

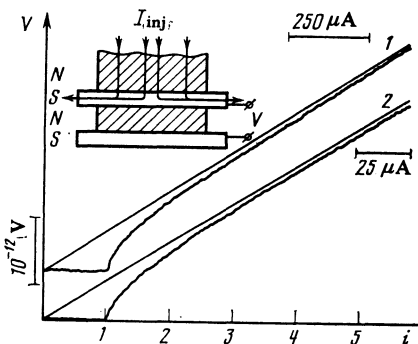


FIG. 3. 1—Voltage across sample No. 1 versus the relative injection current (the experimental geometry is shown in the inset); 2—usual voltage-current characteristic of the Ta-Cu-Ta junction at $T \approx 0.994 T_c$.

essentially the entire cross section of the sample. The period of the oscillations in $I_c(H)$ is $3.5 \cdot 10^{-3}$ Oe, in comparison with a prediction $3.2 \cdot 10^{-3}$ Oe calculated from the dimensions of the junction.

The large dimensions of the junctions mandate a careful screening of the geomagnetic field. A magnetic vacuum no worse than $5 \cdot 10^{-4}$ Oe is achieved with the help of permalloy and niobium superconducting screens.

3. EXCITATION OF JOSEPHSON GENERATION AT AN SNS JUNCTION DURING THE INJECTION OF QUASIPARTICLES INTO ONE SUPERCONDUCTING BANK

In this section we discuss an effect observed during the injection of a quasiparticle current I_{inj} into one of the thin superconducting plates of a junction from a bulk normal layer, with a symmetric removal of the current from the same superconducting plate (see the inset in Fig. 3). The total current across the junction is zero. Curve 1 in Fig. 3 shows the voltage which arises across the junction (sample No. 1) versus the reduced injection current at $T = 0.994 T_c$. The zero on the voltage scale, which corresponds to the steady state of the junction for curve 1 (Fig. 3), has been shifted slightly upward for clarity. The “critical value” of the injection current is nearly ten times the critical value (I_c) of the superconducting transport current I^s through the junction (curve 2), introduced directly through the superconducting plates. Curves 1 and 2 are almost perfectly coincident in the scale shown, but the signs of the voltages measured with identical directions of I_{inj} and I^s are opposite. Curve 2 is the ordinary voltage-current characteristic of a “narrow” ($W \ll \lambda_j$) SNS junction, described by the familiar relation $V = R_n (I^2 - I_c^2)^{1/2}$. (Curves 1 and 2, fitted by the method of least squares, agree with this function with a regression coefficient of 0.999. The asymptotes are drawn on the basis of this calculation.)

Figure 4 shows the voltage across the junction versus the injection of the current found in an experiment in which sample No. 1 was immersed in an alternating magnetic field with a frequency $f = 484$ Hz and an amplitude $\sim 10^{-3}$ Oe. Constant-voltage steps are also observed at $V_N = Nf\Phi_0$ for $N = 1, 2, 3$ when the junction is irradiated by an alternating field at a higher frequency (up to 10 kHz; here Φ_0 is the quantum of magnetic flux). The shape of the curve (Fig. 3) and the observation of constant-voltage steps (Fig. 4) are

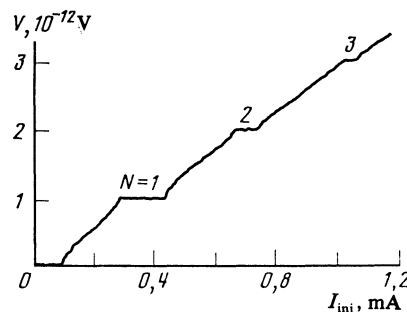


FIG. 4. Voltage across sample No. 1 versus the injection current during irradiation of the junction with an alternating magnetic field with a frequency $f = 484$ Hz ($T = 0.994 T_c$).

reliable evidence that the voltage which arises is of a Josephson nature.

The results will be discussed in detail on the basis of an equivalent circuit for an SNS Josephson junction with banks in a nonequilibrium state in Section 5 below; we restrict the discussion here to a qualitative level.

At temperatures near T_c , the thickness of the superconducting plates (d_S) is comparable to the penetration depth of the electric field (l_E). For this reason, not all of the quasiparticle current which is injected into a bank manages to be converted into a current of pairs over a distance d_S (Fig. 3). As a result, the normal current and the longitudinal electric field penetrate into the region of the weak link and even into the second bank of the junction, where the quasiparticles convert entirely into pairs. The current of quasiparticles across the junction is cancelled by an oppositely directed current of pairs in such a manner that the total current in any cross section of the junction is zero. The magnitude of the supercurrent through a weak link nevertheless determines the onset of a voltage and of Josephson generation in the junction. Similar processes were discussed in Refs. 12–14 for the case of a heat flux through an SNS Josephson junction. In the following section we take up the direct effect of the normal current on the characteristics of the Josephson junction.

Comparing curves 1 and 2 in Fig. 3, we can easily determine d_S/l_E . Since the ratio of the critical currents of these curves is affected somewhat by the magnetic field produced by the large injection current (large in comparison with I_c), we use the linear parts of the curves for the comparison.

4. EFFECT OF THE QUASIPARTICLE CURRENT ON THE CRITICAL CURRENT OF THE SNS JUNCTION

In experiments on the effect of a quasiparticle current on the critical current I_c , two independent transport currents flow simultaneously through the junction, as shown in Fig. 1. The current I_n is injected into the junction through bulk copper plates. The superconducting transport current I^s is injected through the superconducting plates of the junction. In the processing of the experimental data and in the discussion, we take the positive direction of I^s to be that opposite the direction of I^n .

Figure 5 shows two branches of the dependence of the critical transport current (I^s) on the current I^n for sample No. 2 at $T \approx 0.994T_c$. These two curves bound the region of the superconducting state on the phase diagram shown. In a

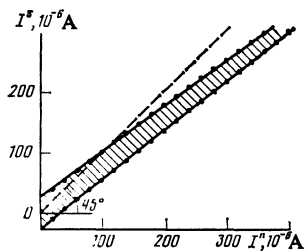


FIG. 5. The critical current (I^s) versus the current I^n for sample No. 2 at $T/T_c = 0.994$. Hatched region—Superconducting state of the junction; unhatched region—resistive state.

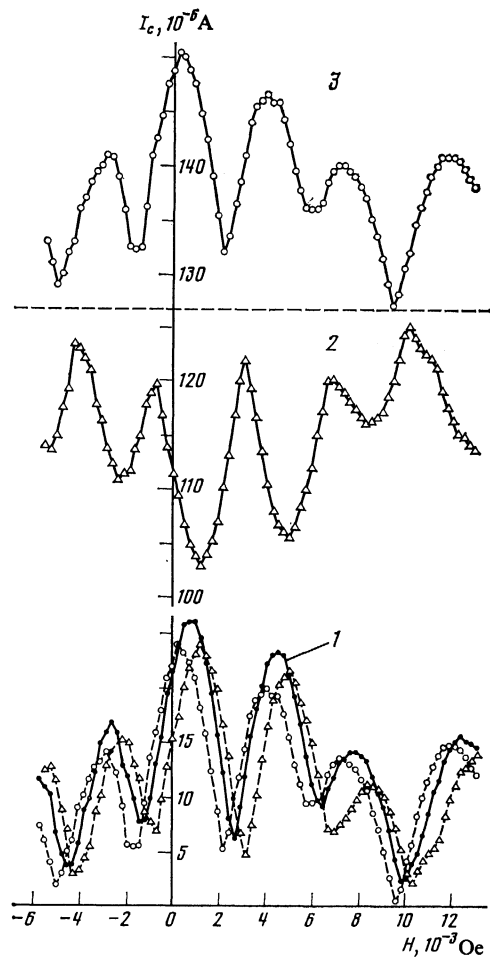


FIG. 6. The critical current I_c (curve 1) for sample No. 2 versus the applied magnetic field. 2, 3—Critical current $(I^2)_c$ versus the field with $I^n = 160 \mu\text{A}$ for the lower and upper branches, respectively (Fig. 5), of the boundary of the resistive state. The dashed line separating curves 2 and 3 corresponds to a zero resultant superconducting current in the sample. The dashed curves in the lower part of the figure are curves 2 and 3, replotted in accordance with relation (1).

zero external magnetic field, the width of the region of the superconducting states, which is $2I_c$ at $I^n = 0$, decreases slightly with increasing I^n . In a certain range of external fields $H \neq 0$ we observe, on the contrary, an increase in the width of the superconducting region. The solid lines in Fig. 6 show the results on (I^s) as a function of H found for sample No. 2 with $I^n = 0$ (curve 1) and $I^n = 160 \mu\text{A}$ at the upper boundary (curve 3) and at the lower boundary (curve 2) of the superconducting state (Fig. 5). The distance between curves 2 and 3 is the width of the superconducting region at $I^n = 160 \mu\text{A}$. The dashed line between the curves corresponds to a zero total supercurrent in the junction. The shape of the $I_c(H)$ curve (at $I^n = 0$) confirms the data from microscopic observations of the nonuniformity of the critical current density along the junction.¹⁸ Let us take a qualitative look at the physical picture which appears in this experiment, postponing a detailed discussion of the results to Section 5.

We first consider the case of a very narrow junction ($W \ll \lambda_J$) with thick ($d_S \gg l_E$) superconducting plates. In a

junction of this sort, all the injected current I^n is converted into a supercurrent in the plate. This supercurrent flows, with a uniform density, through the junction, as does the current I^s injected directly through the superconducting plates. In this case we have a simple addition of the currents I^n and I^s in the junction, and the boundaries of the superconducting region on the phase diagram run parallel to the dashed line shown in Fig. 5, at 45° from the axes. In this particular experimental situation, at $T \approx 0.994 T_c$, the thickness (d_s) of the superconducting plates is comparable to the penetration depth of the electric field (l_E). Consequently, not all of the quasiparticles manage to convert into pairs over the distance d_s , and a normal current $I_n = \alpha I^n$ flows through the junction, where $(1 - \alpha)$ may be described as a coefficient of the conversion of quasiparticles into pairs. Consequently, the total supercurrent through the junction, with the signs of the currents I^n and I^s chosen appropriately, is $[(1 - \alpha)I^n - I^s]$.

Let us assume (Section 5) that the transition to the resistive state occurs when the resultant supercurrent reaches the critical current I_c of the junction. The boundaries of the resistive region are thus determined by

$$(I^s)_c = (1 - \alpha)I^n \pm I_c. \quad (1)$$

Curves of $(I^s)_c$ as a function of I^n and H are shown in Figs. 5 and 6 (curves 1 and 3). The slope of the boundaries of the superconducting region averaged over the magnetic field (Fig. 5) determines α . For sample No. 2 at $T = 0.994 T_c$ we find $\alpha = 0.210$, in good agreement with an independent calculation of α from the relative thickness of the superconducting plate, d_s/l_E , determined for the same sample at the same temperature in the injection experiment described in the preceding section.

It can be concluded from the results shown on the phase diagram in Fig. 5 that the normal component of the current flowing through the Josephson junction, αI^n , has no important effect on the characteristics of the junction. In increasing the current I^n we are simultaneously increasing the normal current αI^n and the supercurrent $(1 - \alpha)I^n$ through the junction. In cancelling the supercurrent with an oppositely directed supercurrent I^s (injected directly through the superconducting plates), we are restoring the junction to a superconducting state. Here the normal current through the junction may be significantly greater than I_c .

To show that the normal current has no effect on the critical current of the junction, we show the curves plotted in Fig. 6 for $I^n = 160 \mu A$ in a different form. Using relation (1), we replot the curves of $(I^s)_c$ versus H as curves of $I_c(H)$ at $I^n = 160 \mu A$ and at the value of α calculated from the injection experiment. The results are shown by the dashed curves in Fig. 6. We are assuming that α is independent of the magnetic field ($< 10^{-2}$ Oe), since it was shown in Ref. 19 that the depth (l_E) to which the electric field penetrates into the superconducting tantalum does not depend on the magnetic field up to 0.1 Oe. It can be seen from a comparison of these curves of $I_c(H)$ that they lie close together. We can conclude from this proximity that the nonequilibrium quasiparticle current has no direct effect on the Joseph-

son characteristics of the junction in a magnetic field. The shift of the curves with respect to each other and with respect to the curve of $I_c(H)$ for $I^n = 0$, and also the change in the width of the superconducting region in Figs. 5 and 6, are due to the effect of the magnetic fields produced by the currents I^n and I^s , which are substantially greater than the critical current I_c of the junction in our experiments. We cannot go into detail here on the manifestations of the effects of the self-magnetic field in these experiments, but we do note that the interaction of a uniform current and a current drawn from the edges of the junction is discussed in Ref. 20.

5. ANALYSIS OF THE RESULTS WITH THE HELP OF AN EQUIVALENT CIRCUIT OF THE JUNCTION

The results obtained here can be understood easily by making use of the equivalent circuit proposed for a nonequilibrium superconductor by Kadin, Smith, and Skocpol.³ Since the SNS Josephson junction has a very small normal resistance ($\sim 10^{-8} \Omega$) and a small characteristic voltage ($I_c R_n \sim 10^{-12}$ V) in our case, the characteristic Josephson frequency is also small (some hundreds of hertz). The inductive and capacitive elements can thus be ignored in the Kadin-Smith-Skocpol equivalent circuit. We are left with the equivalent circuit of the junction shown in Fig. 7. The a^2 blocks represent the superconducting plates of the SNS junction, while R_0 is the resistance of the normal copper intermediate layer. The resistance per unit length of the superconducting plate in the normal state in the direction perpendicular to the plane of the junction is R , while the conductances G represent the channel of the conversion of quasiparticles into a condensate. The resistive line of an a^2 block is the channel for the normal current I_n ; the potential in this line, Φ_n , is the electrochemical potential of the quasiparticles. In turn, the dissipationless line corresponds to the channel for the condensate current I_s ; the potential in this line, $\Phi_s = (\hbar/2e)\chi$, is the electrochemical potential of the Copper pairs, where χ is the phase of the wave function of the corresponding superconducting plate of the junction. The cross represents the region of a pronounced change in the phase χ (the region of the Josephson junction proper), which is reality has a length d_N . [The coherence length $\xi(T)$ in tantalum at $T \approx 0.994 T_c$ is still much smaller than d_s in our case.] We are ignoring the conversion processes in the

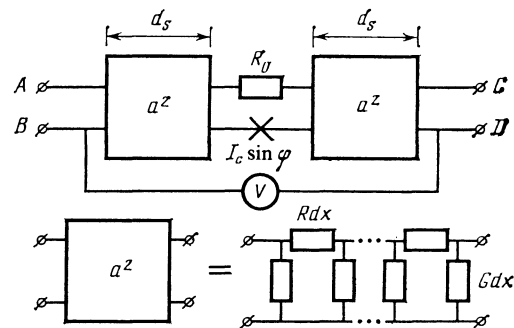


FIG. 7. Equivalent circuit of the junction. a^2 blocks—Superconducting banks of the SNS junction; R_0 —resistance of the copper Josephson intermediate layer; cross—Josephson junction.

region of the normal intermediate layer, since the long energy relaxation time in pure copper would apparently make the contribution of the Josephson copper intermediate layer to this process negligibly small in comparison with that of the tantalum banks. In the experiment, the voltmeter measures the voltage between points *B* and *D*, i.e., the difference between the electrochemical potentials of the pairs, since it is connected by the superconducting contacts to the superconducting plates of the junction.

The physical meaning of an a^2 block is completely clear. Let us assume that a current drawn from the lower line at the right flows into the upper line of the block. This means that a current of quasiparticles is injected into the superconductor from one side, while a supercurrent flows out the other side. The conversion of quasiparticles into pairs does not occur instantaneously at the injection point (such a case would correspond to an infinitely large R or G in the equivalent circuit). Actually, the injected current gradually flows toward the lower line of the a^2 block through conductances G . This conversion of normal current into supercurrent occurs over a region with a scale length l_E . An equation can easily be derived for the current $I_n(x)$ in the upper (normal) line of the a^2 block:

$$d^2 I_n(x)/dx^2 - a^2 I_n(x) = 0, \quad a^2 = RG. \quad (2)$$

On the other hand, we know that the scale depth to which the electric field penetrates into the superconductor due to the imbalance of the populations of the branches of the quasiparticle spectrum is l_E . It is thus natural to define G in such a manner that we have $a = l_E^{-1}$. We have hence

$$a/G = Rl_E, \quad l_E = (RG)^{-1/2}. \quad (3)$$

Solving Eq. (2) with various boundary conditions, we can analyze all the experiments. We also use an expression for the voltage at an arbitrary point x_0 between the normal and superconducting lines of the equivalent circuit in the form $U(x_0) = -(1/G)dI_n/dx$, where $U(x_0)$ is the difference between the electrochemical potentials of the pairs and quasiparticles at x_0 . We turn now to the analysis of the experiments.

1. A current introduced into the SNS junction through the superconducting contacts corresponds to the equivalent circuit to a current I^s which flows into point *B* and out of point *D*. The current at points *A* and *C* is taken to be zero. From Eq. (2) and the boundary conditions we find the following equation for the phase difference across the Josephson junction, $\varphi(t)$:

$$\frac{\hbar}{2eR_n} \dot{\varphi} + I_c \sin \varphi = I^s, \quad R_n = R_0 + \frac{2Rl_E}{\text{th } d_s/l_E}. \quad (4)$$

Here d_s is the thickness of the superconducting electrode. This result is completely understandable physically: The effective resistance of the junction, R_n , in this case is simply the resistance of the normal intermediate layer (R_0) and the excess resistance of the superconducting plates which stems from the penetration of the electric field to a depth l_E into these plates.

It follows from (4) that the voltage-current characteristic is described by

$$V = R_n [(I_s)^2 - I_c^2]^{1/2}. \quad (5)$$

2. Let us examine now the injection experiment described in Section 3. In terms of our equivalent circuit, we inject a direct current I_{inj} at contact *A* and extract the same current at contact *B*. The currents at *C* and *D* are zero. The equivalent circuit makes it a simple matter to understand the physical processes in this experiment. The normal current injected into the superconducting plate must turn into a supercurrent which is removed from the same plate. For this purpose, there must be a conversion of quasiparticles into Copper pairs, which can occur only over a scale depth l_E . If $d_s \sim l_E$, the conversion of normal current into supercurrent continues all the way to the second superconducting plate of the junction, and a normal current flows through resistance R_0 in the direction toward this plate. The equal supercurrent must return, since the total of the junction must be zero. If the oppositely directed supercurrent exceeds I_c , the voltmeter begins to show a voltage, and its sign must be opposite that of the voltage which arises when a current flows completely through the junction (by virtue of the opposite direction of the supercurrent). This is precisely what we saw experimentally.

Simple calculations based on Eq. (2) lead to the following equation for the injection case:

$$\frac{\hbar}{2eR_n} \dot{\varphi} + I_c \sin \varphi = \frac{I_{inj} Rl_E}{R_n \text{sh } d_s/l_E}. \quad (6)$$

This equation means that the critical injection current—the current at which a voltage appears at contacts *B* and *D*—is

$$(I_{inj})_c = I_c \frac{R_n \text{sh } d_s/l_E}{Rl_E}. \quad (7)$$

From Eq. (6) we also find the dependence of V on I_{inj} :

$$V = R_{inj} [(I_{inj})^2 - (I_{inj})_c^2]^{1/2}, \quad R_{inj} = Rl_E/\text{sh } d_s/l_E. \quad (8)$$

In order to compare the voltage-current characteristics of the junction for the case in which a current flows completely through the superconducting contacts, (5), and in the injection experiment, (8), we write the current in these equations in a form normalized to the corresponding critical current:

$$V = R_n I_c (i_s^2 - 1)^{1/2}, \quad i_s = I^s/I_c, \quad (5')$$

$$V = R_n I_c (i_{inj}^2 - 1)^{1/2}, \quad i_{inj} = I_{inj}/(I_{inj})_c. \quad (8')$$

Expressed in these units, the two voltage-current characteristics should evidently coincide, and again this is what we observe experimentally (Fig. 3).

Let us use relation (7) to estimate the factor by which the critical injection current $(I_{inj})_c$ exceeds the critical current of the junction, I_c . For sample No. 1 (for which the results were discussed in Section 3), the thickness of the superconducting plates is about $3.5 \cdot 10^{-4}$ cm, the area of the junction is $2 \cdot 10^{-2}$ cm², the normal resistivity of the tantalum plates is $0.77 \cdot 10^{-6}$ Ω·cm, the resistance of the normal intermediate layer is (estimated to be) $R_0 = 1.0 \cdot 10^{-9}$ Ω, and the total resistance of the junction (for $T/T_c \simeq 0.994$) is R_n

$\approx 2 \cdot 10^{-8} \Omega$. Using (4), we can estimate the depth to which the electric field penetrates at the experimental temperature: $l_E \approx 2 \cdot 10^{-4}$ cm. From (7) we then find $(I_{inj})_c / I_c = 6$. The experimental value of this ratio is 6.5.

3. The introduction of a current into the junction through the normal contacts corresponds to the specification of a current I^n at contacts A and C . Solving Eq. (2) under these boundary conditions, we find

$$\frac{\hbar}{2eR_n} \dot{\varphi} + I_c \sin \varphi = I^n \left(1 - \frac{2Rl_E}{R_n \operatorname{sh} d_s / l_E} \right). \quad (9)$$

This result means that the critical current of the junction in this case is

$$(I^n)_c = I_c \left(1 - \frac{2Rl_E}{R_n \operatorname{sh} d_s / l_E} \right)^{-1}.$$

It also follows from (9) that under the condition $I^n < (I^n)_c$ (i.e., in the steady state) the supercurrent flowing directly through the Josephson junction is

$$I_s = I_c \sin \varphi = I^n \left(1 - \frac{2Rl_E}{R_n \operatorname{sh} d_s / l_E} \right). \quad (10)$$

This result means that the supercurrent I_s and a quasiparticle current (a normal current) flow simultaneously through the SNS junction. The condition $I_s < I_c$ means that the junction is in a steady state, i.e., the voltage across the junction (the reading of the voltmeter connected to the superconducting electrodes of the junction) is zero. Nevertheless, a quasiparticle current flows through the junction, and if we connected the voltmeter to points A and C in the equivalent circuit we would observe a nonzero voltage. For this purpose we would have to connect the normal potentiometer leads to the superconducting electrodes of the junction; i.e., we would have to measure the difference in electrochemical potentials of the quasiparticles.

It follows from (10) that the fraction of the normal current which flows in a dissipationless regime through resistance R_0 is

$$\alpha = \frac{I^n - I_s}{I^n} = \frac{2Rl_E}{R_n \operatorname{sh} d_s / l_E}. \quad (11)$$

In our experiments, the product αI^n could be very large, reaching values three or four times the critical current of the junction, I_c . The supercurrent caused at the junction by the current I^n may have been completely cancelled by the opposite supercurrent injected through the superconducting electrodes. As a result, the situation may have been such that the total supercurrent across the junction was zero, and only the normal current αI^n flowed across it. The junction would then be in a steady state (Fig. 5).

Let us use (11) to evaluate α for sample No. 2 at the temperature of the experiment described in Section 4. Sample No. 2 differs from sample No. 1, for which estimates were made above, only in the area of the junction (about $1.5 \cdot 10^{-2}$ cm²) and the thickness of the superconducting plates, $d_s \approx 4 \cdot 10^{-4}$ cm. The value of α for this junction should be 0.24. This value agrees well with the experimental result $\alpha \approx 0.21$ given in Section 4. It thus follows from this discussion of the results that the Kadin-Smith-Skocpol equivalent circuit,³

simplified somewhat to correspond to our case, gives a good description of an SNS Josephson junction under nonequilibrium conditions.

The following experimental results are of particular interest. As we already mentioned in Section 4 and in the discussion of Eq. (10), an experimental situation was possible in which a large normal current $\alpha I^n > I_c$ flowed through the junction, while the supercurrent was zero, and the system was in a steady state (Fig. 5). A similar effect was observed in the case in which the junction was in a magnetic field, and Josephson vortices penetrated into it. We must therefore conclude that the normal current flowing through the SNS junction does not interact with the Josephson vortices. A different situation arises in our injection experiments (Section 3). The total current through the junction is zero in this case; nevertheless, when the injection current exceeds a critical value $(I_{inj})_c$ a resistive state appears, Josephson generation begins, and—in the presence of a magnetic field—the motion of Josephson vortices begins. An analogous situation has been observed in experiments on thermoelectric effects at SNS Josephson junctions.¹²⁻¹⁴ Again in those experiments, a Josephson generation and a motion of vortices began when the heat flux through the junction exceeded a critical value. In both cases, however, a supercurrent flowed through the junction while the total current was zero.

Putting all these experiments together, we find a rather nontrivial result: Only a supercurrent interacts with Josephson vortices; the quasiparticle current does not interact with them (at least under our experimental conditions).

6. TEMPERATURE DEPENDENCE OF I_E OF THE SUPERCONDUCTING PLATES

Study of the temperature dependence of the observed effects yields the temperature dependence of the depth (l_E) to which the longitudinal electric field penetrates into the superconducting plates of the junction. There are two independent ways to find this temperature dependence: by studying the temperature dependence of the fraction of the normal current (α) and using (11) or by studying the temperature dependence of the resistance ratio R_{inj} / R_n on the basis of the linear region of voltage-current characteristics like those in Fig. 3. Using (8) and (4), and ignoring $R_0 \ll R_n$, we find the following result for temperatures near T_c :

$$R_{inj} / R_n = 1/2 \operatorname{ch} (d_s / l_E). \quad (12)$$

It is easy to see that the ratio of differential resistances corresponding to the linear parts of the curves found during the injection of quasiparticles and during the introduction of a current directly through the superconducting plates is determined by the ratio d_s / l_E .

Since the critical current of the junction increases, and the Josephson penetration depth λ_J correspondingly decreases, as the temperature is lowered, the junction ceases to be "narrow"; i.e., its width W becomes greater than λ_J . As a result, the boundaries of the resistive state (Fig. 5) cease to be linear, and self-modulation effects arise on the injection voltage-current characteristic (Fig. 3) because of the effect of the self-magnetic field of the large injection current. For

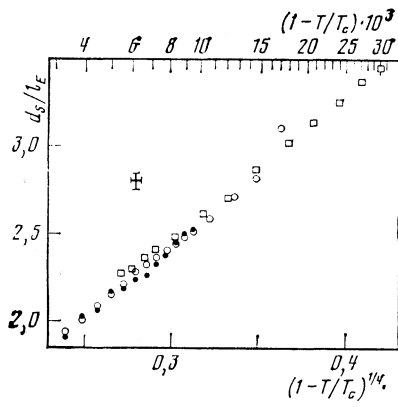


FIG. 8. Temperature dependence of the reduced thickness (d_s/l_E) of a superconducting bank of the SNS junction. \circ —Calculated from the fraction (α) of the normal current for sample No. 2 [see (11)]; \bullet —calculated from the ratio of the resistance R_{inj} during the injection of quasiparticles into one superconducting bank to the junction resistance R_n for sample No. 2 [see (12)]; \square —the same, for sample No. 3.

this reason, it was difficult to study the temperature dependence of l_E for samples Nos. 1 and 2 at comparatively low temperatures. To expand the temperature range, the change in l_E was also carried out for sample No. 3, with a thicker normal Josephson intermediate layer ($d_N \approx 5.5 \mu\text{m}$) and with a correspondingly smaller critical current.

The experimental results are shown in Fig. 8 as a plot of d_s/l_E versus $(1 - T/T_c)^{1/4}$. There is a clearly expressed linear behavior at temperatures near T_c , up to $0.97T_c$. This result means that the observed effects are determined over a broad temperature range by the value of l_E , whose temperature dependence is described by^{1,11}

$$l_E = 2 \left(\frac{lv_F}{9.3\pi} \tau_e \right)^{1/2} (1 - T/T_c)^{-1/4}, \quad (13)$$

where l is the electron mean free path, v_F is the Fermi velocity, and τ_e is the electron-phonon energy relaxation time in tantalum. This time is easily determined from the slope of the plot in Fig. 8. The value found, $\tau_e \approx 4 \cdot 10^{-11}$ s, differs slightly from that found in Ref. 16: $\tau_e \approx 1 \cdot 10^{-10}$ s. The discrepancy can be attributed to the greater accuracy of the method used in the present experiments and also to the higher quality of the superconducting contacts, which improves the accuracy with which the critical current of tantalum and the ratio T/T_c are determined. Another possibility is that the discrepancy stems from the different deformations of the tantalum during the fabrication of samples with thin and thick superconducting plates.

In Ref. 16, τ_e was determined from the excess resistance of non-Josephson Ta-Cu-Ta junctions, which is proportional to $(1 - T/T_c)^{-1/4}$ at temperatures $T > 0.994T_c$. At lower temperatures, the Andreev reflection of quasiparticles at the NS interface sharply reduces the number of quasiparticles which penetrate into the superconductor. This changed the temperature dependence of the excess resistance and made it possible to study the conversion in the mass of the superconductor only in a narrow temperature interval. Despite the fact that the Andreev reflection begins to affect the excess resistance of our samples at a temperature $T \approx 0.992T_c$, it is

easy to see that the curves in Fig. 8 are linear over the entire temperature range studied, all the way to $T > 0.997T_c$. A distinctive feature of these experiments is that here we are interested in the fraction of the quasiparticles injected into the superconducting plate which passes into the normal Josephson intermediate layer of the junction. Since there are two oppositely acting NS interfaces in the path of the quasiparticles here, the Andreev reflection has a weak effect on the magnitude of the normal current in the Josephson junction.

It was shown in Ref. 1 that if the superconductor and the normal metal have identical characteristics (Fermi velocities, electron mean free paths, electrical conductivities, etc.), the jump (δE) in the electric field at the NS interface is given by the expression

$$\delta E = 1/4 (3\pi)^{1/2} (\Delta/T)^{1/2} (l_e/l)^{1/4} E_S, \quad (14)$$

where E_S is the electric field on the side of the superconductor, l_e is the energy relaxation length of the electrons, and Δ is the energy gap.

This result means that if a normal current is flowing through an NS interface, and if its magnitude on the side of the normal metal is J_n , then its value changes abruptly at the interface to the value of the normal current on the side of the superconductor, J_{ns} ; here we have

$$J_{ns} = \beta J_n. \quad (15)$$

The value of β is easily found from (14):

$$\beta = [1 + 1/4 (3\pi)^{1/2} (\Delta/T)^{1/2} (l_e/l)^{1/4}]^{-1}. \quad (16)$$

A calculation based on the Kadin-Smith-Skocpol circuit with the auxiliary boundary conditions in (15) leads to the following expression [which is analogous to (4)] for the junction resistance R_n^* :

$$R_n^* = R_0 + \frac{2Rl_E\beta}{\text{th } d_s/l_E}, \quad (4')$$

This expression determines the excess resistance¹ with allowance for Andreev reflection. We see that the value of β directly affects the junction resistance. The fraction of the normal current, α , is now given by an expression analogous to (11):

$$\alpha = \frac{I^n - I_s}{I^n} = \frac{2Rl_E\beta}{R_n^* \text{sh } d_s/l_E} = \frac{1}{\text{ch } d_s/l_E} \left(1 + \frac{R_0 \text{th } d_s/l_E}{2Rl_E\beta} \right)^{-1} \quad (11')$$

When Andreev reflection is taken into account, expression (8) for R_{inj} becomes $R_{inj}^* = Tl_E\beta / \sinh(d_s/l_E)$, and the ratio R_{inj}^*/R_n^* becomes

$$\frac{R_{inj}^*}{R_n^*} = \frac{1}{2 \text{ch } d_s/l_E} \left(1 + \frac{R_0 \text{th } d_s/l_E}{2Rl_E\beta} \right)^{-1} \quad (12')$$

Analysis of (11') and (12') shows that Andreev reflection begins to have a noticeable influence on these effects under the condition $\beta < R_0/2Rl_E$. At $T = 0.997T_c$ we have $R_0/2Rl_E \approx 0.1$, and an estimate of β from the excess resistance yields $\beta \sim 0.5$ [an estimate from (16) is approximately the same], so that Andreev processes in the temperature range studied should not have any strong influence on the effects studied here. This conclusion agrees with the experimental results (Fig. 8).

Finally, we should point out that the conditions for the applicability of (14) and (16) to the tantalum-copper pair were discussed in Ref. 16. Furthermore, a more accurate calculation of the magnitude of the jump in the electric field at the *NS* interface, incorporating the difference between the properties of the normal metal and the superconductor, does not change the conclusions drawn above in any essential way.

7. CONCLUSION

In summary, we have developed a procedure for injection experiments to study the effect of a nonequilibrium flow of quasiparticles on the properties of *SNS* Josephson junctions. We have shown that even in the absence of a total current through the junction the injection of quasiparticles into one of the superconducting banks gives rise to Josephson generation. Taken together, the experimental results show that a nonequilibrium quasiparticle flow has no direct effect on the Josephson characteristics of the junction. The appearance of a difference in the electrochemical potentials of the pairs and of generation at the junction is due exclusively to the flow of a superconducting current.

The good quantitative agreement between the experimental results and calculations based on the Kadin-Smith-Skocpol equivalent circuit (simplified somewhat) proves that this circuit is a suitable model for accurately describing nonequilibrium processes in a superconductor.

Study of the temperature dependence of various properties shows that Andreev reflection has no important influence on the effects found here over a rather broad temperature range. The methods which have been proposed thus make it possible to study nonequilibrium processes in the interior of a superconductor at temperatures lower than is possible by means of, for example, the method of studying the excess resistance of *SNS* sandwiches.

We are indebted to K. K. Likharev for a discussion of this paper and to N. S. Stepanov for assistance in the preparation for the experiments.

- ¹S. N. Artemenko and A. F. Volkov, *Usp. Fiz. Nauk* **128**, 3 (1979) [*Sov. Phys. Usp.* **22**, 295 (1979)].
- ²T. Y. Hsiang and J. Clarke, *Phys. Rev.* **21B**, 945 (1980).
- ³A. M. Kadin, L. N. Smith, and W. J. Skocpol, *J. Low Temp. Phys.* **38**, 497 (1980).
- ⁴A. M. Kadin, C. Varmazis, and J. E. Lukens, *Physica (Utrecht)* **107B**, 159 (1981).
- ⁵M. L. Yu and J. E. Mercereau, *Phys. Rev. Lett.* **28**, 1117 (1972).
- ⁶J. Clarke, *Phys. Rev. Lett.* **28**, 1363 (1972).
- ⁷J. Bindslev Hansen and P. E. Lindelof, *Rev. Mod. Phys.* **56**, 431 (1984).
- ⁸K. K. Likharev, *Vvedenie v dinamiku dzhozefsonovskikh perekhodov* (Introduction to the Dynamics of Josephson Junctions), Ch. 13, Nauka, Moscow, 1985.
- ⁹M. A. H. Horenberg, J. A. Blackburn, and D. W. Jillie, *Phys. Rev.* **21B**, 125 (1980).
- ¹⁰J. A. Blackburn, *J. Low Temp. Phys.* **50**, 475 (1983).
- ¹¹A. Schmid and G. Schön, *J. Low Temp. Phys.* **20**, 207 (1975).
- ¹²M. V. Kartsovnik, V. V. Ryazanov, and V. V. Schmidt, *Pis'ma Zh. Eksp. Teor. Fiz.* **33**, 373 (1981) [*JETP Lett.* **33**, 356 (1981)].
- ¹³V. V. Ryazanov and V. V. Schmidt, *Solid State Commun.* **40**, 1055 (1981).
- ¹⁴G. I. Panaitov, V. V. Ryazanov, A. V. Ustinov, and V. V. Schmidt, in: *LT-17 Proceedings* (ed. V. Eckern, A. Schmid, W. Weber, and H. Wühl), Part II, 1984, p. 823.
- ¹⁵V. K. Kaplunenko and V. V. Ryazanov, *Phys. Lett.* **110A**, 145 (1985).
- ¹⁶V. V. Ryazanov, V. V. Schmidt, and L. A. Ermolaeva, *J. Low Temp. Phys.* **45**, 507 (1981).
- ¹⁷T. Y. Hsiang and D. K. Finnemore, *Phys. Rev.* **22B**, 154 (1980).
- ¹⁸A. Barone and G. Paterno, *The Physics and Applications of the Josephson Effect*, Wiley-Interscience, 1981 (Russ. transl. Mir, Moscow, Ch. 4, 1984).
- ¹⁹G. Yu. Logvenov and V. V. Ryazanov, *Fiz. Nizk. Temp.* **9**, 933 (1983) [*Sov. J. Low Temp. Phys.* **9**, 481 (1983)].
- ²⁰V. V. Ryazanov and A. V. Ustinov, *Fiz. Nizk. Temp.* **11**, 909 (1985) [*Sov. J. Low Temp. Phys.* **11**, No. 9 (1985)].

Translated by Dave Parsons